Title

Understanding the structure of isolated iridium sites anchored on a covalent triazine framework

Journal

Catalysis Science & Technology, 13(9)

ISSN

2044-4753

Authors

Sackers, Nina M
Iemhoff, Andree
Sautet, Philippe
et al.

Publication Date

2023-05-09

DOI

10.1039/d3cy00232b

COMMUNICATION

Understanding the structure of isolated iridium sites anchored on a covalent triazine framework

Received 00th January 20xx,
Accepted 00th January 20xx

DOI: 10.1039/x0xx00000x

Nina M. Sackers,[a] Andree Iemhoff,[a] Philippe Sautet [b,c] and Regina Palkovits [a]*

As a showcase for experimentally accessible single-site catalysts, well-defined and characterized isolated Ir sites anchored on a covalent triazine framework (CTF) were investigated with computational methods. The resting states of the catalyst species after immobilization as well as after reduction at 400 °C could be identified. These resting states were found to not be the catalytically active species but pre-catalysts for the dehydrogention of formic acid.

Heterogeneous single-site and single-atom catalysts currently gain increasing attention in combining the high activity of homogeneous catalysts with the robustness of heterogeneous catalysts.[1-6] Among the carbon-based support materials for immobilized metal species, CTFs represent a very promising material class due to their tuneable properties such as the electronic structure or the porosity based on the choice of the organic linker (Figure 1).[7] Moreover, the high amount of nitrogen functionalities make CTFs a suitable support for anchoring metal species.[8]

Various applications for catalysts based on metal species immobilized on CTFs have already been reported.[7, 8] For example, Pt/CTF was used as a heterogeneous analogue to the Periana catalyst and showed similar activity for the oxidation of methane to methanol as well as high stability under acidic conditions.[9] For the oxidation of biomass-derived chemicals such as 5-hydroxymethylfurfural, a Ru salt was anchored on CTF and reduced to Ru^0, which outperformed the commercial Ru/C catalyst.[10] Moreover, an Ir pentamethylcyclopentadienyl (Cp*) precursor was immobilized on a CTF support and achieved a turn-over frequency (TOF) of up to 27000 h^{-1} for the hydrogen formation from formic acid (FA).[11]

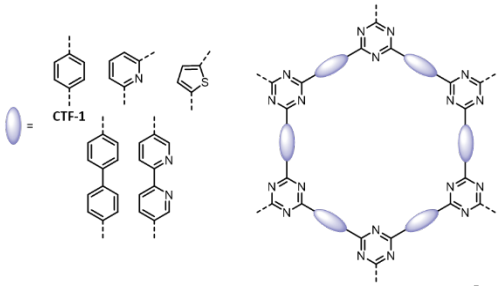

Figure 1: Schematic structure of a CTF and potential organic linkers.[7]

Recently, Iemhoff et al. reported isolated iridium species immobilized on the so-called 'CTF-1' that catalyse the dehydrogenation of FA as a model reaction.[12] As this catalyst material is structurally well defined and experimentally quite well understood, it was chosen as a case study for the herein reported computational analysis of heterogeneous single-atom catalysts using periodic density functional theory calculations.

Experimentally, two catalytically active species were obtained. After immobilization of an Ir(acac)(COD) (acac = acetyl-acetonate, COD = 1,5-cyclooctadiene) precursor, the catalyst achieved a TOF of 16900 h^{-1} for the FA dehydrogenation (FADH) in aqueous solution. However, this material lacks stability as it loses 88% of its activity after recycling the catalyst five times. If the immobilized Ir/CTF species is reduced at 400 °C before catalytic experiments, a higher initial TOF of 24400 h^{-1} is obtained. In addition, this material possesses a higher selectivity by forming less CO and an improved stability in recycling experiments. Despite the differences in activity, both catalyst materials are composed of isolated Ir atoms, as extended X-ray absorption fine structure (EXAFS) results confirmed the absence of Ir-Ir bonds. Reduction of Ir/CTF at higher temperatures above 400 °C however, results in formation of Ir nanoparticles.[12]

[a] *Chair of Heterogeneous Catalysis and Technical Chemistry, ITMC, RWTH Aachen University, Worringerweg 2, 52074 Aachen, Germany. *E-mail: Palkovits@itmc.rwth-aachen.de*
[b] *Department of Chemical and Biomolecular Engineering, University of California, Los Angeles, California 90095, United States.*
[c] *Department of Chemistry and Biochemistry, University of California, Los Angeles, California 90095, United States.*

Electronic Supplementary Information (ESI) available: [Computational details, adsorption geometries and energies, XRD spectra, Bader charge densities, (P)DOS, energy profiles]. See DOI: 10.1039/x0xx00000x

With this contribution, we provide computational insights into the catalyst structure of isolated Ir species on a CTF macroligand and compare these findings to the experimental characterization by Iemhoff et al.[12] Starting from modelling of the CTF support, the resting states of the catalyst species after impregnation with an Ir precursor and after reductive pre-treatment are identified. Finally, a first modelling of the FADH on the reduced Ir/CTF is performed by deriving catalytic cycles to determine the activity.

The pristine CTF-1 was modelled in a 2D layered structure. Comparing simulated X-ray diffraction (XRD) spectra of different stackings to experimental findings[12] revealed that the CTF is constructed of either perfect AA stacking comprising congruent CTF layers or slightly shifted AA stacked layers (Figure S1). This shifted AA stacking has the triazine N above the triazine C of the next CTF layer and shows a better stability than the perfect AA stacking (Figure S1), which can probably be explained by reduced electrostatic repulsion between the Ns of the layers. Despite lower stability, the CTF with perfect AA stacking matches the experimental cell parameters determined by Liu et al.[13] better (Table S1).

As IR studies suggested, a ligand exchange of the COD ligand from the Ir(acac)(COD) precursor upon coordination to the CTF macroligand and the interaction of Ir and the CTF N was experimentally confirmed by X-ray photoelectron spectroscopy (XPS)[12]. Accordingly, potential anchoring points of Ir(acac) on the CTF that contain Ir-N interactions were investigated for the immobilized Ir species. Ir(acac) was placed on top of the CTF slab and between two CTF layers resulting in interaction with N from both CTF layers (Figure S2, a-d). In addition, the Ir species was inserted into the C-H bond of the support's phenyl ring while simultaneously interacting with N from the same CTF layer (Figure 2, Figure S2, e). This adsorption geometry turned out to be the most favourable structure (Figure S3). Similar structures could already be observed for molecular iridium bipyridinyl complexes.[14, 15] In accordance with experiment by Iemhoff et al.[12], this geometry contains interaction of Ir with N and has a formal oxidation state of +III, which coincides with the white line intensity in X-ray absorption spectroscopy (XAS) suggesting an Ir(III) species. Consequently, this structure corresponds to the resting state after immobilization of the Ir precursor. Similar structures with one O of the acac ligand detached from the Ir were found less stable (Figure S2, f-g). The same applies to the coordination of acac via the carbon atom (Figure S2, h-i).

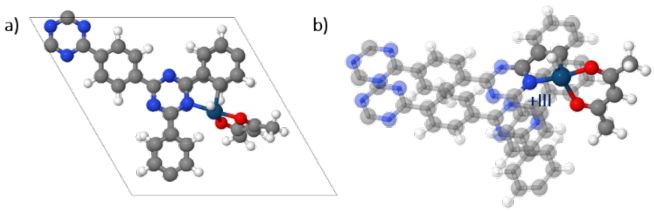

Figure 2: Most stable adsorption geometry of Ir(acac) on CTF in a) front view and b) side view. Formal oxidation state of Ir denoted in blue.

To derive a catalytic cycle for the FADH on this catalyst model, adsorption studies of potential intermediates (carboxyl + H, formate + H) and the reactant FA were performed. However, all tested geometries were found extremely unfavourable and exclude the possibility of an energetically reasonable catalytic cycle (Figure S4, Table S2). Equally unfavourable adsorption energies were observed for slightly modified structures that reduce the repulsion at the Ir centre (Table S3). For example, one of the O from the acac ligand was detached from the Ir centre or the hydride ligand at the Ir centre was transferred to the acac resulting in an acetylacetone ligand or the corresponding enol form. This leads to the conclusion that the computationally determined most stable resting state structure for Ir(acac)/CTF is not the catalytically active structure. Instead, the catalyst centre might undergo fundamental restructuring during the catalytic experiments that might include ligand exchange. The weak recyclability of the catalyst supports this hypothesis.

After reduction at 400 °C, the Ir sites remain isolated according to annular dark-field scanning transmission electron microscopy (ADF-STEM) results, but IR measurements indicate that the acac ligand is removed from the Ir.[12] In addition, near edge X-ray absorption fine structure (NEXAFS) studies suggest the formation of an Ir-C bond.[12] Consequently, various adsorption sites for the bare Ir atom on CTF were tested (Figure S5). The most stable geometry is quite similar to Ir(acac)/CTF and contains N coordination as well as C-H activation and Ir-C and Ir-H coordination. However, these interactions take place within two CTF layers (Figure S6), which is in good agreement with the EXAFS fit (Table S4). To account for the reductive conditions, the hydrogenation stage of Ir was investigated. Despite an excess of hydrogen, the most stable geometry contains one H less than the naked Ir and CTF (Figure 3). This geometry contains the four-fold coordination of Ir as proposed by EXAFS and matches the distances for the first and second coordination sphere (Table S4). Moreover, the formal oxidation state +III suits the experimental white line intensity in XAS[12] and this structure resembles a reasonable product from the hydrogenolysis of the acac ligand in Ir(acac)/CTF. For a similar material based on Cu single atoms immobilized in a carbon nitride support, Vilé et al. also studied such a sandwich-like structure.[16] However, in their case the investigated interaction of Cu with three layers of the support was found to not match the experimental XAS data well.

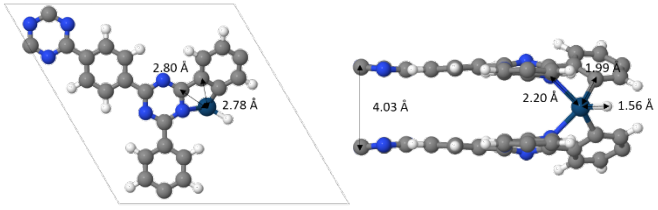

Figure 3: Front and side view of the most stable Ir/CTF after reductive treatment at 400 °C and removal of the acac ligand by hydrogenolysis.

A comparison of XRD data of the pure CTF and Ir/CTF after reduction reveals significant changes for larger 2Θ angles (Figure S8). A loss of short-range order can be suspected from disappearing reflects at 12.5° and 25° and a simultaneous increase of the signal around 24.5° corresponding to amorphous carbon.[17-19] This could be due to local hydrogenation resulting in tilting of the aromatic rings through

formation of sp^3 instead of sp^2 carbon. The long-range order however, seems to be maintained, as the reflect at 7° is unaffected. Despite its high activity for reducing its environment, Ir itself is more stable in a less reduced position (cf. Figure S7). Consequently, after catalysing the hydrogenation of its environment, Ir would migrate through the CTF to such less reduced site. Therefore, modifications of the CTF support might not be in the direct environment of the Ir and should have a minor influence on the active centre.

Regarding the electronic structure of the two catalyst materials, a slight decrease in the partial positive charge of Ir can be observed for Ir/CTF compared to the precursor complex, while Ir(acac)/CTF has a more positive charge (Table S5). This coincides with the XPS results of a higher electron density at Ir after reductive treatment.[12] Moreover, Bader analysis revealed that the coordinating N atoms in Ir/CTF and Ir(acac)/CTF donate electron density to the Ir centre. While pristine CTF has localized states at the Fermi level arising from lone pairs of the N atoms (Figure S9), these states are quenched upon interaction with Ir (Figure S10). This behaviour is even more pronounced for the Ir(acac)/CTF system, which could be due to a more favourable geometric arrangement of the Ir interaction with only one CTF layer.

Similar to Ir(acac)/CTF, the reduced Ir/CTF (Figure 3) was found to be an unsuitable catalyst model for the FADH, as no local minima could be identified for the interaction with substrate or intermediates. To enable the interaction with the substrate, an additional adsorption site on the Ir centre was created by migration of the H initially on Ir and recovery of the phenyl C-H bond (Figure S11). This geometry is destabilized only by about 30 kJ mol^{-1} and requires an activation energy of about 50 kJ mol^{-1} (Figure S12).

For both investigated pathways of the catalytic cycles for FA to CO_2 via formate (HCOO, Figure S13) and carboxyl (COOH, Figure S14), the dehydrogenation steps were found to require the highest activation barriers between 80 – 170 kJ mol^{-1}, while the barriers for rotation of intermediates are rather low (< 30 kJ mol^{-1}). Overall, rather high energetic spans (ESs) are observed for both pathways, with the reaction sequence via the carboxyl intermediate being slightly preferred over the formate pathway (Table 1). At a reaction temperature of 160 °C, these ESs correspond to TOFs in a range of 10^{-6} – 10^{-4} h^{-1}. A comparison to the experimental TOF for the FADH in aqueous solution reveals a difference in up to ten orders of magnitude and emphasizes that the investigated model is inactive for FADH. Even though this is only a rough estimate, as not all experimental conditions such as the presence of water are considered, the discrepancy between calculation and experiment is large. In order to reach a TOF similar to experiment, the ES would have to be reduced to about 100 kJ mol^{-1} (Table 1). This reduction cannot be achieved by a modification of the investigated catalytic cycles (Figures S13-14).

Table 1: ESs and corresponding TOFs determined for the FADH on Ir/CTF.[a]

Pathway	ES [kJ mol^{-1}]	TOF [h^{-1}]
Formate	182	$3.67 \cdot 10^{-6}$
Carboxyl	163	$7.17 \cdot 10^{-4}$
Experimental[12]	(101)	24400

[a] Value in brackets indicates an ES calculated from experimental TOF.

However, it has to be emphasized that the comparability of computational and experimental results in this study is rather weak. One reason is the neglect of the solvent in the computations. Especially polar solvents such as water have a great influence on the mechanism and the activation barriers.[20] Consequently, either the solvent has to be considered in the calculations or the experimental catalytic tests need to be performed in the gas phase. Moreover, modelling at different length scales is required for a comprehensive comparison to experiment.[21]

Nevertheless, the large difference between experimental and computational reactivity reveals that the slight modification of the Ir/CTF resting state does not lead to the active site. Instead, bigger structural changes than the recovery of the C-H bond have to take place. The active state could be obtained from reductive activation with H_2 from the Ir/CTF resting state. For example, adding two H_2 would result in a species that has the Ir coordinated to only one CTF layer (Figure S7, +3 H). This species might be more reactive due to less repulsive interactions of the ligands.

In summary, with a combination of computational modelling and extensive analytical methods, the resting states of the immobilized Ir(acac)/CTF and the Ir/CTF after reductive pre-treatment could be identified. However, assuming only minimal changes in the structure of the resting state is not sufficient to depict the catalytically active species under experimental conditions. Consequently, further efforts have to be made to reveal the experimentally active geometry. In this context, *in situ* XAS experiments for the characterization of the actual active site would be the most reasonable starting point. A realistic model of the catalytically active site could also explain the high selectivity for FADH with regard to the CO formation. This result could coincide with a preference for the dehydrogenation reaction via the formate pathway, as the formation of CO from carboxyl should be predominant.[22] Finally, this investigation shows that computational chemistry can confirm experimental findings and provide insights into the catalyst structure. Moreover, these results prove that reliable computations and experiments go hand in hand.

Acknowledgement

This work was performed as part of the Cluster of Excellence Fuel Science Center (EXC 2186, ID: 390919832) funded by the Excellence Initiative by the German federal and state governments to promote science and research at German universities. NMS thanks RWTH Aachen University for financial support. We thank Isabella Kappel for measuring XRD samples

as well as Christopher Zurek, Julius Stockmann and Kelly Tran for their contributions to the calculations.

Conflicts of interest

There are no conflicts to declare.

Notes and references

1 J. M. Thomas, R. Raja and D. W. Lewis, *Angew. Chem. Int. Ed.*, 2005, **44**, 6456-6482.
2 A. Wang, J. Li and T. Zhang, *Nat. Rev. Chem.*, 2018, **2**, 65-81.
3 M. Heitbaum, F. Glorius and I. Escher, *Angew. Chem. Int. Ed.*, 2006, **45**, 4732-4762.
4 J. Liu, *ACS Catal.*, 2017, **7**, 34-59.
5 X.-F. Yang, A. Wang, B. Qiao, J. Li, J. Liu and T. Zhang, *Acc. Chem. Res.*, 2013, **46**, 1740-1748.
6 S. Liang, C. Hao and Y. Shi, *ChemCatChem*, 2015, **7**, 2559-2567.
7 J. Artz, *ChemCatChem*, 2018, **10**, 1753-1771.
8 A. Iemhoff, M. Vennewald and R. Palkovits, *Angew. Chem. Int. Ed.*, 2022, e202212015.
9 R. Palkovits, M. Antonietti, P. Kuhn, A. Thomas and F. Schüth, *Angew. Chem. Int. Ed.*, 2009, **48**, 6909-6912.
10 J. Artz, S. Mallmann and R. Palkovits, *ChemSusChem*, 2015, **8**, 672-679.
11 A. V. Bavykina, M. G. Goesten, F. Kapteijn, M. Makkee and J. Gascon, *ChemSusChem*, 2015, **8**, 809-812.
12 A. Iemhoff, M. Vennewald, J. Artz, C. Mebrahtu, A. Meledin, T. E. Weirich, H. Hartmann, A. Besmehn, M. Aramini and F. Venturini, *ChemCatChem*, 2022, **14**, e202200179.
13 M. Liu, K. Jiang, X. Ding, S. Wang, C. Zhang, J. Liu, Z. Zhan, G. Cheng, B. Li and H. Chen, *Adv. Mater.*, 2019, **31**, 1807865.
14 K. J. Young, M. Yousufuddin, D. H. Ess and R. A. Periana, *Organometallics*, 2009, **28**, 3395-3406.
15 L. Cancela, M. A. Esteruelas, A. M. López, M. Oliván, E. Oñate, A. San-Torcuato and A. Vélez, *Organometallics*, 2020, **39**, 2102-2115.
16 G. Vilé, G. Di Liberto, S. Tosoni, A. Sivo, V. Ruta, M. Nachtegaal, A. H. Clark, S. Agnoli, Y. Zou and A. Savateev, *ACS Catal.*, 2022, **12**, 2947-2958.
17 E. Kim and R. Patel, *Membr. J.*, 2021, **31**, 184-199.
18 C. Amorim, G. Yuan, P. M. Patterson and M. A. Keane, *J. Catal.*, 2005, **234**, 268-281.
19 S. Kuecken, J. Schmidt, L. Zhi and A. Thomas, *J. Mater. Chem. A*, 2015, **3**, 24422-24427.
20 L. Yu, X. Pan, X. Cao, P. Hu and X. Bao, *J. Catal.*, 2011, **282**, 183-190.
21 B. W. Chen, L. Xu and M. Mavrikakis, *Chem. Rev.*, 2020, **121**, 1007-1048.
22 J. A. Herron, J. Scaranto, P. Ferrin, S. Li and M. Mavrikakis, *ACS Catal.*, 2014, **4**, 4434-4445.

